Simultaneous Transfer and Doping of CVD-Grown Graphene by Fluoropolymer for Transparent Conductive Films on Plastic

Wi Hyoung Lee,[†,§] Ji Won Suk,[†] Jongho Lee,[‡] Yufeng Hao,[†] Jaesung Park,[§] Jae Won Yang,[§] Hyung-Wook Ha,[†] Shanthi Murali,[†] Harry Chou,[‡] Deji Akinwande,[‡] Kwang S. Kim,[§] and Rodney S. Ruoff[†,*]

[†]Department of Mechanical Engineering and the Materials Science and Engineering Program, The University of Texas at Austin, Austin, Texas 78712, United States, [‡]Department of Electrical and Computer Engineering, Microelectronics Research Center, The University of Texas at Austin, Austin, Texas 78758, United States, and [§]Center for Superfunctional Materials, Department of Chemistry, Pohang University of Science and Technology, Pohang 790-784, Korea

Graphene receives considerable attention in part because of its electrical, mechanical, thermal, and optical properties.[1−5] Its use as a transparent conductive graphene electrode fabricated on plastic substrate is targeted for commercialization.[6−10] The DC to optical conductivity ratio is used as a figure of merit for transparent conductive electrodes (TCE).[8] Although chemically derived graphene (*i.e.*, reduced graphene oxide or colloidal sheets exfoliated from graphite, *etc.*) can be used to fabricate a low-cost and large-area conductive film, their DC to optical conductivity ratio is not as good as chemical vapor deposition (CVD)-grown graphene.[8,11,12] Large-area graphene films grown by CVD on metal foils are promising and depend on the transfer of the graphene from the metal to a target substrate.[13−16] CVD-grown graphene on Cu foil combined with polymer-supported or roll-to-roll transfer of the graphene can yield a relatively high DC to optical conductivity ratio near that of commercial indium tin oxide (ITO) electrodes.[7,14]

One issue is the effect of polymer residues on the properties of graphene.[17−22] Polymer residues are reported to remain on the graphene surface during the transfer and patterning of the CVD-grown graphene.[17,18,23] Although thermal annealing particularly in ultra-high vacuum (UHV) is a possible method to remove these residues,[24] most of the plastic substrates on which the graphene would be deposited for TCE application cannot survive such high temperature annealing and use of UHV is cost prohibitive. Thus, it is necessary to reveal how these

ABSTRACT
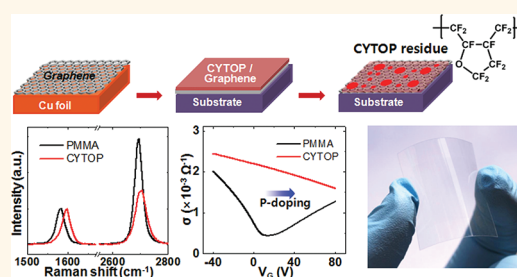
Chemical doping can decrease sheet resistance of graphene while maintaining its high transparency. We report a new method to simultaneously transfer and dope chemical vapor deposition grown graphene onto a target substrate using a fluoropolymer as both the supporting and doping layer. Solvent was used to remove a significant fraction of the supporting fluoropolymer, but residual polymer remained that doped the graphene significantly. This contrasts with a more widely used supporting layer, polymethylmethacrylate, which does not induce significant doping during transfer. The fluoropolymer doping mechanism can be explained by the rearrangement of fluorine atoms on the graphene basal plane caused by either thermal annealing or soaking in solvent, which induces ordered dipole moments near the graphene surface. This simultaneous transfer and doping of the graphene with a fluoropolymer increases the carrier density significantly, and the resulting monolayer graphene film exhibits a sheet resistance of ∼320 Ω/sq. Finally, the method presented here was used to fabricate flexible and a transparent graphene electrode on a plastic substrate.

KEYWORDS: graphene transfer · transparent conductive film · field-effect transistor · doping · fluoropolymer

polymer residues affect the electrical properties of the graphene through doping and distinguish that from the unintentional doping from other atmospheric adsorbates while achieving a better understanding of the doping mechanism.[25] Another issue is reducing the sheet resistance of the graphene while maintaining high transparency.[8] One current method induces charge transfer
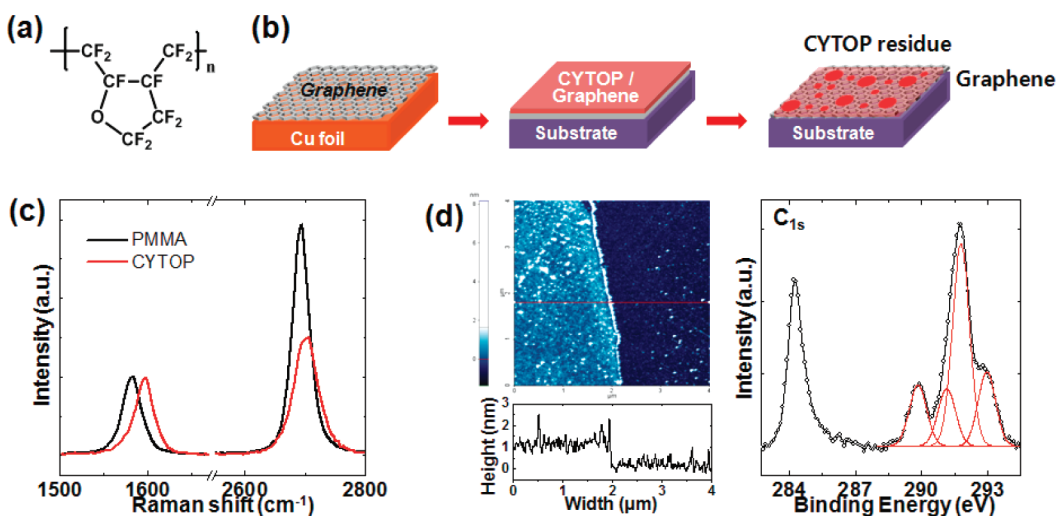
Figure 1. (a) Chemical structure of CYTOP. (b) Schematic of the graphene transfer process with CYTOP supporting layer. (c) Raman spectra of the graphene films transferred onto SiO_2/Si substrates with PMMA (black) or CYTOP (red) as the supporting layer. (d) AFM image ($4 \times 4\,\mu m$) (left) and XPS C_{1s} spectrum (right) of the graphene film having an ultrathin CYTOP residue layer on the top surface. Bottom inset of the AFM image shows the cross-sectional profile.

between graphene and dopant molecules with $AuCl_3$ or metal nanoparticles to increase the carrier density of the graphene.[26−28] However, these materials are rather expensive, so a facile, simple, inexpensive doping method would be beneficial. Furthermore, this method should be compatible with plastic substrates.

We developed a new method to simultaneously transfer and dope CVD-grown graphene onto a target substrate. A fluoropolymer was used as both the supporting and doping layer in the transfer of the graphene. The doping properties of the fluoropolymer and polymethylmethacrylate (PMMA) were compared through Raman spectroscopy and electrical characterization. Furthermore, this method was used to fabricate a transparent conductive film on a plastic substrate.

RESULTS AND DISCUSSION

Graphene films were transferred onto target substrates using two different supporting layers, PMMA and a fluoropolymer (CYTOP from Asahi glass, Figure 1a). Figure 1b shows the schematic transfer processes of the graphene films, which consists of polymer coating, Cu etching, polymer/graphene pick-up, thermal annealing at 140 °C, and polymer removal. Both PMMA and CYTOP proved to be successful for graphene transfer. When CYTOP was used, strong graphene doping was confirmed by a decrease of I_{2D}/I_G and blue shifts of G and 2D bands (Figure 1c).[29,30] The atomic force microscopy (AFM) image on the left of Figure 1d shows that a residual CYTOP layer of 1−2 nm in thickness covers the entire graphene surface. The X-ray photoelectron spectroscopy (XPS) spectrum, as shown on the right of Figure 1d, also confirms that a residual CYTOP layer covers the graphene surface. Four distinct features corresponding to the structural elements of

CYTOP, C−F (289.8 eV), O−C−F (291.1 eV), $C−F_2$ (291.8 eV), and $O−C−F_2$ (293.0 eV) groups, appeared along with the sp^2-hybridized graphene peak at 284.2 eV in the C_{1s} spectrum. The graphene peak shifts to lower binding energy compared to the pristine graphene or graphite peak, which is due to the p-doping of the graphene by the CYTOP residue.[7,23,31] This residue remains on the graphene surface even after a long soaking time (∼3 days) in solvent. Similarly, an ultrathin PMMA residue on the graphene surface was observed in AFM images when PMMA was used instead;[19] it dopes graphene much less than the CYTOP residue, as shown below.

The graphene films were transferred onto silicon nitride (SiN_x) membranes that contain an array of $3\,\mu m$ diameter holes to exclude the effect of doping of substrate and thus to investigate the effect of polymer residues on the intrinsic doping of graphene (see Supporting Information Figure S1 for the image of a membrane).[32−34] Micro-Raman spectra prove that the CYTOP supporting layer leads to a high doping level even in freestanding graphene film. When the films were annealed at 500 °C to decompose the CYTOP residue, the graphene film is no longer doped. This is confirmed by the red shifts of the G and 2D bands and the abrupt increase of I_{2D}/I_G. However, the graphene film transferred by PMMA showed a small increase in intensity of the 2D band and no significant changes in the peak positions. Figure 2b shows plots for the position of the G band *versus* I_{2D}/I_G of the Raman spectra in the supported films (Figure 1c) and the freestanding films (Figure 2a). The supported graphene films show higher doping levels compared to the freestanding films. This means that the substrate and/or adsorbates on the substrate can also dope the graphene films and confirms that the choice of
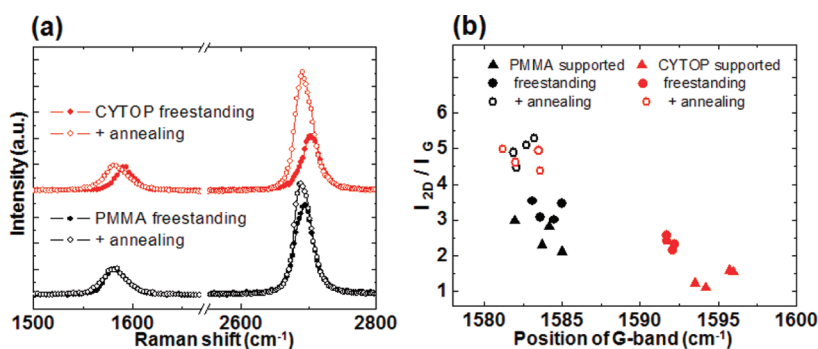
Figure 2. (a) Raman spectra of freestanding graphene films transferred onto SiN$_x$ membranes with PMMA (black) or CYTOP (red) as the supporting layer. (b) Comparative plots for the position of the G band *versus* ratio of intensity of the 2D band over the G band (closed triangle, as-transferred graphene films supported on SiO$_2$/Si substrates; closed circles, as-transferred freestanding graphene films; open circles, freestanding graphene films after thermal annealing at Ar/H$_2$ condition, 400 °C (PMMA) or 500 °C (CYTOP) for 2 h).
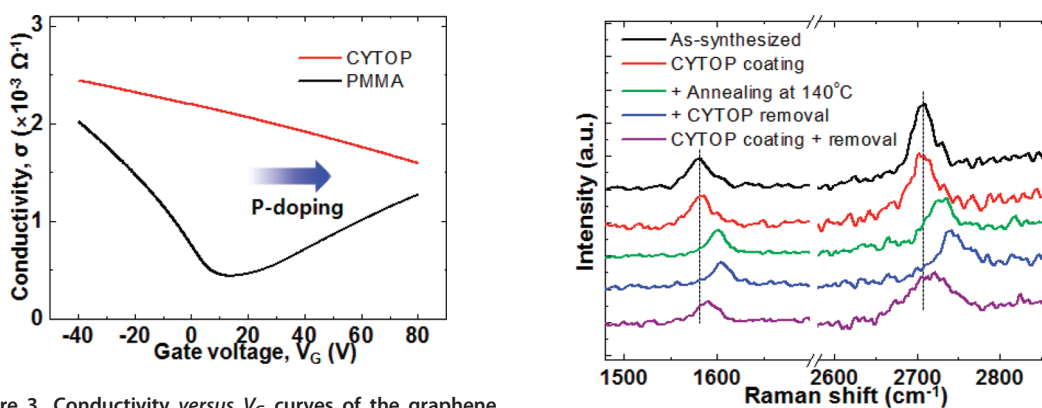

Figure 3. Conductivity *versus* V_G curves of the graphene FETs constructed on SiO$_2$/Si substrates with PMMA (black) or CYTOP (red) as the supporting layer.

Figure 4. Change of the Raman spectra in the graphene films on Cu foils after coating with CYTOP, then thermal annealing at 140 °C, and finally after removal of most of the CYTOP with solvent (black, as-synthesized graphene films on Cu foils; red, after coating with a thin CYTOP layer; green, after coating with a thin CYTOP layer and thermal annealing at 140 °C; blue, after coating with a thin CYTOP layer, thermal annealing at 140 °C and then removing thin CYTOP layer with solvent; purple, after coating with thin CTTOP layer and subsequently removing the thin CYTOP layer with a solvent).

the substrate also modulates the graphene doping level.[32,35−37] It is notable that the Raman data of both freestanding films transferred by PMMA and by CYTOP after annealing are similar. By effectively eliminating the contributors to doping from the top and bottom surfaces of the graphene by the use of the suspended structure and thermal annealing, the transferred graphene films exhibited nearly the same quality of freestanding graphene prepared by mechanical exfoliation.[32] However, for the practical application of graphene in TCE, the graphene should be supported on a substrate and, at least for many substrates, should not be annealed at high temperature. Thus, polymer residues will remain on the graphene, and choosing the supporting layer for transfer is an important consideration to achieve the desired function.

Figure 3 shows the electrical properties of graphene field-effect transistors (FETs), which exhibit strikingly different performance depending on the residual polymer type. The Dirac point voltage (V_{Dirac}), where the carrier type is changed, is regarded as an indicator for the type of doping and the concentration of excess charge carriers.[38,39] For the graphene FETs with PMMA residue, V_{Dirac} is placed around 10 V. On the other hand, the graphene FETs with CYTOP residue exhibit no

detectable V_{Dirac} even when the gate voltage is swept to 100 V, which is near the breakdown voltage of the SiO$_2$ (285 nm) layer. This proves that the graphene film with CYTOP residues is significantly p-doped. The slightly positive value of V_{Dirac} in the graphene film with PMMA residues might be due to doping by charged impurities present on the SiO$_2$ surface (below the graphene) and/or H$_2$O and O$_2$ molecules adsorbed on the PMMA residue on the graphene.[25,36,40,41] The carrier mobilities were calculated for the linear regime using the following equation:[39]

$$\mu = \frac{1}{C_i}\frac{d\sigma}{dV_G} \qquad (1)$$

where $C_i = 1.1 \times 10^{-8}$ F cm^{-2}.

The hole and electron mobilities of graphene FETs with PMMA residue (average over 18 devices) were 2700 and 970 cm^2/(V·s), and the hole mobility of
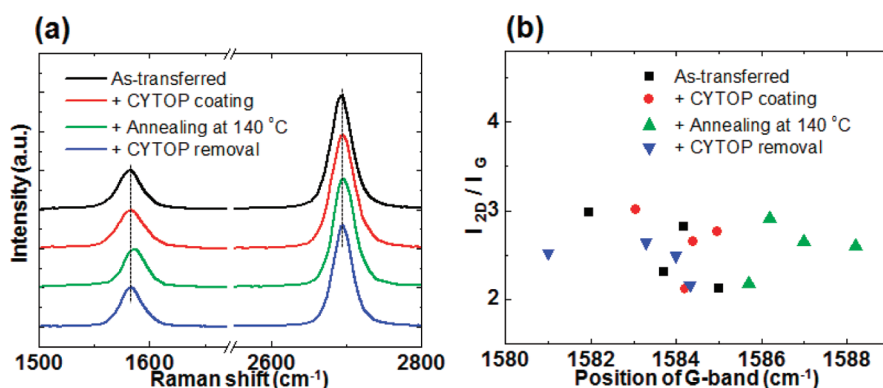
Figure 5. (a) Change of the Raman spectra in the graphene films (transferred with a PMMA supporting layer) after CYTOP coating, then thermal annealing at 140 °C, and finally after removal of most of the CYTOP with a solvent. (b) G band position *versus* ratio of intensity of the 2D band over the G band (black, as-transferred graphene films supported on SiO_2/Si substrates; red, after coating with a thin CYTOP layer; green, after thermal annealing at 140 °C; blue, after removing most of the thin CYTOP layer with a solvent).

graphene FETs with CYTOP residue (average over 10 devices) was 810 cm^2/(V·s). The decrease in field-effect mobility demonstrates that CYTOP residue induces an uneven doping profile, thereby causing scattering of the charge carriers.[42]

To further examine the doping characteristics, Raman spectra of the graphene films on Cu foils were taken after coating them with a thin CYTOP layer (~10 nm) (Figure 4). The peak position (G and 2D) and I_{2D}/I_G did not change. Subsequent thermal annealing at 140 °C, however, led to abrupt blue shifts in the G and 2D bands arising from p-doping of the graphene. After removing most of the CYTOP layer with solvent, the G and 2D bands shifted even more, indicating that the magnitude of p-doping increased slightly. In a parallel experiment, p-doping of the graphene is also observed when the spin-coated CYTOP layer is directly removed with solvent before thermal annealing. The absence of doping immediately after deposition of the CYTOP layer implies that some residual solvent or the intimate contact between CYTOP and the graphene is not the reason for the doping. It is known that charge transfer doping is determined by the energy difference between the work function of the graphene and the electron affinity of the acceptor molecules or the ionization potential of the donor molecules.[28,43] However, this concept is not applicable in the CYTOP/ graphene system because CYTOP is an insulating polymer and the electron affinity of the CYTOP is not larger than the work function of the graphene, and therefore, contact of CYTOP onto graphene does not induce significant graphene doping in the *ab initio* calculations (see Supporting Information Figures S2 and S3 and text). We suggest that graphene doping can be induced by the electrostatic potential created by the dipole moment. This concept has been previously used to explain doping by self-assembled monolayers (SAMs) on monolayer graphene with multilayer regions prepared by mechanical exfoliation.[44,45]

Although the CVD process is used to synthesize monolayer graphene, multilayer regions of 2–10% coverage are inevitably formed on Cu foil (see Supporting Information Figure S4). Thus, doping by SAMs has also been observed on CVD-grown monolayer graphene.[31,46] Similar to SAMs, functional groups in polymers can induce an ordered dipole moment as far as there is an alignment of the functional groups.[47] However, the fluorine atoms in CYTOP likely exhibit a random orientation after spin-coating, and thus graphene film exhibits nearly undoped characteristics (Figure 4). It is considered that thermal annealing at 140 °C or soaking in solvent can enhance the movement of polymer chains and encourage rearrangement of the fluorine atoms toward the graphene basal plane. Such a dipole moment near the graphene surface would lead to a large downward shift of the Fermi level and result in p-doping of the graphene. To support this idea, the graphene film was placed on a CYTOP film by transferring the graphene film with PMMA supporting layer. In this control experiment, doping was only observed in the graphene film after thermal annealing (see Supporting Information Figure S5). We speculate that the interaction between the graphene and the fluorine atoms might be the reason for the local alignment of fluorine atoms directed toward the graphene basal plane and into an ordered dipole moment. In this context, thermal annealing of the CYTOP before graphene contact may not induce a dipole moment within the CYTOP layer. Thus, the graphene transferred onto a thermally treated CYTOP layer does not exhibit any significant doping (see Supporting Information Figure S6). It should be noted that the CYTOP layer affecting the doping is restricted to only within several molecular layers of the graphene where there is an ordered dipole moment. Thus, the magnitude of doping measured by the Raman spectra does increase slightly after removing the 10 nm thick CYTOP layer with solvent (Figure 4). Note that soaking in solvent to remove the CYTOP layer may increase
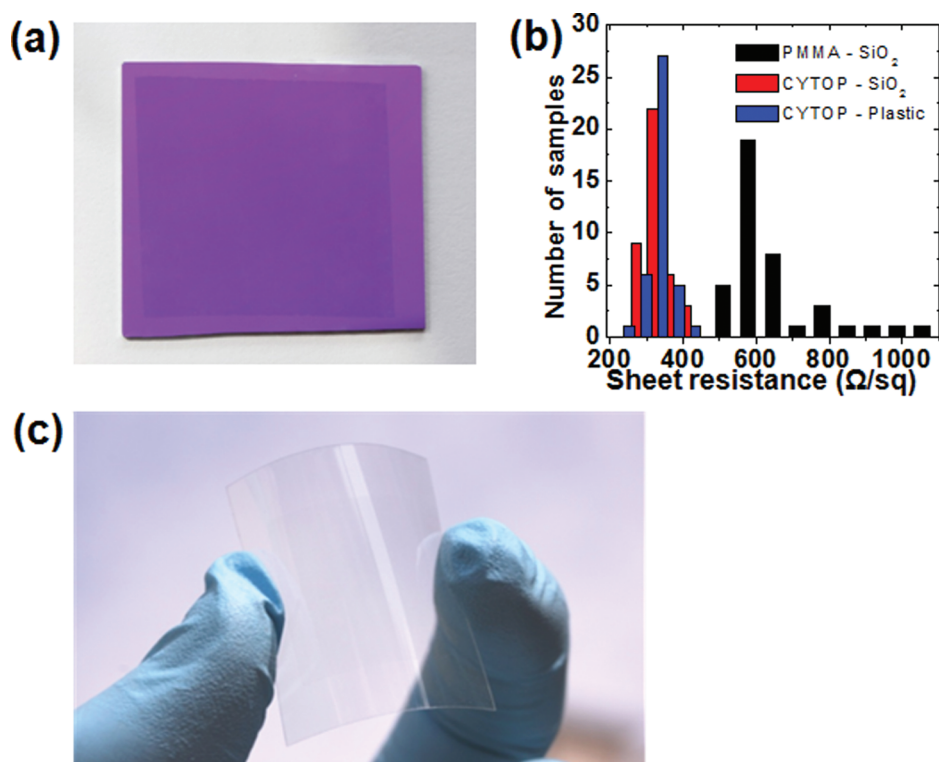
LEE *ET AL.*   VOL. 6 ▪ NO. 2 ▪ 1284–1290 ▪ 2012 ACSNANO **1287**

www.acsnano.org

Figure 6. (a) Digital camera image of the graphene film transferred onto a SiO₂/Si substrate with a CYTOP supporting layer. (b) Sheet resistances of graphene films transferred using PMMA or CYTOP. (c) Digital camera images of the graphene film on a PET substrate transferred with a CYTOP supporting layer having high transparency and flexibility.

rearrangement of the fluorine atoms where an ultrathin residue layer of thickness around 1–2 nm remains on the graphene surface (Figure 1d).

The key idea in this report is the "simultaneous transfer and doping of graphene in a one-step process". As a comparison, a PMMA-transferred graphene film was subsequently coated with a thin CYTOP layer (~10 nm) to dope the graphene film. Figure 5 shows the change in the Raman spectra of the graphene films after CYTOP coating, thermal annealing at 140 °C, and CYTOP removal with solvent. The position of the G band shifts slightly after CYTOP coating and thermal annealing at 140 °C, whereas I_{2D}/I_G does not change much. This contrasts with the significant graphene doping, as shown in Figure 1c and Figure 4. Consider that the CYTOP layer does not contact the graphene surface directly, but rather an ultrathin PMMA residue. Thus, doping is not facilitated due to the PMMA residue between the graphene and CYTOP. Furthermore, the position of the G band in the graphene film after removing the CYTOP layer recovers to the original value before any CYTOP coating. The interaction between the graphene and CYTOP might be weakened by the presence of a PMMA residue covering the graphene surface, and thus the CYTOP layer can be easily removed during soaking in solvent and the doping effect disappears. Contrary to our results, doping of the graphene films transferred with supporting polymer was successful when strong acids (*i.e.*, HNO₃,

HCl) were used as dopants.[7] We speculate that a strong acid can dope graphene by permeating through and simultaneously removing the PMMA. We used a CYTOP film for transfer and doping of graphene in a one-step process, which might reduce processing costs.

Sheet resistances of the graphene electrodes transferred with two different supporting layers (PMMA, CYTOP) were measured. A clean image with uniform optical contrast in Figure 6a suggests that CYTOP is a good candidate for the large-area transfer of CVD-grown graphene. Plots for the sheet resistances from 40 different positions are shown in Figure 6b. The graphene films transferred with a CYTOP supporting layer exhibit an average sheet resistance of 320 ± 37 Ω/sq, lower than that of PMMA (650 ± 160 Ω/sq). This is due to the doping of the graphene by a residual CYTOP layer. Furthermore, sheet resistance of the graphene transferred by CYTOP shows no change after one month. This is due to the stable doping of the graphene by CYTOP. Because the solvent to dissolve CYTOP does not damage the plastic substrate, the graphene film with low sheet resistance (340 ± 32 Ω/sq) was successfully fabricated on a PET substrate, and high transparency and flexibility are shown in Figure 6c. The graphene films transferred by this method might find use in organic field-effect transistors and organic solar cells where the formation of a multilayer is critical to the performance of the devices.

CONCLUSIONS

In summary, a simple doping method has been developed using CYTOP as a simultaneous transfer and doping layer for CVD-grown graphene. The graphene sheet resistance is significantly reduced because of an ultrathin residual CYTOP layer which p-dopes the graphene; doping from a residual PMMA layer is not as high as from a CYTOP layer. The CYTOP doping mechanism can be explained by the rearrangement of fluorine atoms on the graphene basal plane caused either by thermal annealing or by soaking in solvent, which induces ordered dipole moments near the graphene surface. The method presented here can be used to fabricate flexible and transparent graphene electrodes because of the simplicity of this doping process and its compatibility with plastic substrates.

EXPERIMENTAL SECTION

Graphene Transfer and Device Fabrication. Monolayer graphene films containing 2−10% multilayer regions were synthesized using the CVD process reported in our previous paper.[14] The as-grown graphene films on copper foil were then flattened by pushing the films between two cover glass slides, covered with PMMA (M_w = 996 kg mol^{-1}) or fluoropolymer (Cytop, Asahi Glass Co.) and floated in a 0.05 M ammonium persulfate ((NH_4)$_2S_2O_8$) solution. After all of the copper had been etched away, the graphene films were transferred to either SiO$_2$/Si, SiN$_x$ membrane, or polyethylene terephthalate (PET) substrates. Thermal annealing at 140 °C was used to remove residual solvent and increase interaction between the graphene and the polymer. The graphene films remained on the substrates after removing the supporting layers with solvent. To define source/drain electrodes for graphene field-effect transistors (FETs), Cr (5 nm)/Au (60 nm) was thermally evaporated through a shadow mask (channel length = 30 μm, channel width = 500 μm) onto a SiO$_2$ (thickness of 285 nm)/Si wafer.

Characterization. The graphene films were characterized with optical microscopy (Zeiss Axioskop), atomic force microscopy (AFM, PSIA model XE-1000S), scanning electron microscopy (SEM, FEI Quanta 600), and micro-Raman imaging spectroscopy (WiTec Alpha, 488 nm laser wavelength). The graphene surface with residual polymer was analyzed by measuring X-ray photoelectron spectra using a Kratos AXIS Ultra DLD spectrometer. The sheet resistances of the graphene films were measured by the van der Pauw four-probe method (Keithley 6221 and 6514 instruments). The current−voltage characteristics of the graphene FETs were analyzed using an Agilent semiconductor parameter analyzer.

Supporting Information Available: Figures S1−S6 and the results of *ab initio* calculations. This material is available free of charge *via* the Internet at http://pubs.acs.org.

Conflict of Interest: The authors declare no competing financial interest.

REFERENCES AND NOTES

1. Zhang, Y. B.; Tan, Y. W.; Stormer, H. L.; Kim, P. Experimental Observation of the Quantum Hall Effect and Berry's Phase in Graphene. *Nature* **2005**, *438*, 201–204.
2. Novoselov, K. S.; Geim, A. K.; Morozov, S. V.; Jiang, D.; Katsnelson, M. I.; Grigorieva, I. V.; Dubonos, S. V.; Firsov, A. A. Two-Dimensional Gas of Massless Dirac Fermions in Graphene. *Nature* **2005**, *438*, 197–200.
3. Lee, C.; Wei, X. D.; Kysar, J. W.; Hone, J. Measurement of the Elastic Properties and Intrinsic Strength of Monolayer Graphene. *Science* **2008**, *321*, 385–388.
4. Zhu, Y. W.; Murali, S.; Cai, W. W.; Li, X. S.; Suk, J. W.; Potts, J. R.; Ruoff, R. S. Graphene and Graphene Oxide: Synthesis, Properties, and Applications. *Adv. Mater.* **2010**, *22*, 5226–5226.
5. Allen, M. J.; Tung, V. C.; Kaner, R. B. Honeycomb Carbon: A Review of Graphene. *Chem. Rev.* **2010**, *110*, 132–145.
6. Li, X. S.; Zhu, Y. W.; Cai, W. W.; Borysiak, M.; Han, B. Y.; Chen, D.; Piner, R. D.; Colombo, L.; Ruoff, R. S. Transfer of Large-Area Graphene Films for High-Performance Transparent Conductive Electrodes. *Nano Lett.* **2009**, *9*, 4359–4363.
7. Bae, S.; Kim, H.; Lee, Y.; Xu, X.; Park, J.-S.; Zheng, Y.; Balakrishnan, J.; Lei, T.; Kim, H. R.; Song, Y. I.; *et al.* Roll-to-Roll Production of 30-in. Graphene Films for Transparent Electrodes. *Nat. Nanotechnol.* **2010**, *5*, 574–578.
8. De, S.; Coleman, J. N. Are There Fundamental Limitations on the Sheet Resistance and Transmittance of Thin Graphene Films? *ACS Nano* **2010**, *4*, 2713–2720.
9. Hecht, D. S.; Hu, L. B.; Irvin, G. Emerging Transparent Electrodes Based on Thin Films of Carbon Nanotubes, Graphene, and Metallic Nanostructures. *Adv. Mater.* **2011**, *23*, 1482–1513.
10. Feng, X. L.; Pang, S. P.; Hernandez, Y.; Mullen, K. Graphene as Transparent Electrode Material for Organic Electronics. *Adv. Mater.* **2011**, *23*, 2779–2795.
11. Park, S.; Ruoff, R. S. Chemical Methods for the Production of Graphenes. *Nat. Nanotechnol.* **2009**, *4*, 217–224.
12. Eda, G.; Chhowalla, M. Chemically Derived Graphene Oxide: Towards Large-Area Thin-Film Electronics and Optoelectronics. *Adv. Mater.* **2010**, *22*, 2392–2415.
13. Reina, A.; Jia, X. T.; Ho, J.; Nezich, D.; Son, H. B.; Bulovic, V.; Dresselhaus, M. S.; Kong, J. Large Area, Few-Layer Graphene Films on Arbitrary Substrates by Chemical Vapor Deposition. *Nano Lett.* **2009**, *9*, 30–35.
14. Li, X. S.; Cai, W. W.; An, J. H.; Kim, S.; Nah, J.; Yang, D. X.; Piner, R.; Velamakanni, A.; Jung, I.; Tutuc, E.; Banerjee, S. K.; Colombo, L.; Ruoff, R. S. Large-Area Synthesis of High-Quality and Uniform Graphene Films on Copper Foils. *Science* **2009**, *324*, 1312–1314.
15. Kim, K. S.; Zhao, Y.; Jang, H.; Lee, S. Y.; Kim, J. M.; Kim, K. S.; Ahn, J. H.; Kim, P.; Choi, J. Y.; Hong, B. H. Large-Scale Pattern Growth of Graphene Films for Stretchable Transparent Electrodes. *Nature* **2009**, *457*, 706–710.
16. Cai, W. W.; Zhu, Y. W.; Li, X. S.; Piner, R. D.; Ruoff, R. S. Large Area Few-Layer Graphene/Graphite Films as Transparent Thin Conducting Electrodes. *Appl. Phys. Lett.* **2009**, *95*, 123115/1–123115/3.
17. Cheng, Z. G.; Zhou, Q. Y.; Wang, C. X.; Li, Q. A.; Wang, C.; Fang, Y. Toward Intrinsic Graphene Surfaces: A Systematic Study on Thermal Annealing and Wet-Chemical Treatment of SiO$_2$-Supported Graphene Devices. *Nano Lett.* **2011**, *11*, 767–771.
18. Lin, Y. C.; Jin, C. H.; Lee, J. C.; Jen, S. F.; Suenaga, K.; Chiu, P. W. Clean Transfer of Graphene for Isolation and Suspension. *ACS Nano* **2011**, *5*, 2362–2368.
19. Ishigami, M.; Chen, J. H.; Cullen, W. G.; Fuhrer, M. S.; Williams, E. D. Atomic Structure of Graphene on SiO$_2$. *Nano Lett.* **2007**, *7*, 1643–1648.
20. Chen, C. Y.; Rosenblatt, S.; Bolotin, K. I.; Kalb, W.; Kim, P.; Kymissis, I.; Stormer, H. L.; Heinz, T. F.; Hone, J. Performance of Monolayer Graphene Nanomechanical Resonators with Electrical Readout. *Nat. Nanotechnol.* **2009**, *4*, 861–867.

21. Dan, Y. P.; Lu, Y.; Kybert, N. J.; Luo, Z. T.; Johnson, A. T. C. Intrinsic Response of Graphene Vapor Sensors. *Nano Lett.* **2009**, *9*, 1472–1475.

22. Pettes, M. T.; Jo, I. S.; Yao, Z.; Shi, L. Influence of Polymeric Residue on the Thermal Conductivity of Suspended Bilayer Graphene. *Nano Lett.* **2011**, *11*, 1195–1200.

23. Lee, W. H.; Park, J.; Sim, S. H.; Lim, S.; Kim, K. S.; Hong, B. H.; Cho, K. Surface-Directed Molecular Assembly of Pentacene on Monolayer Graphene for High-Performance Organic Transistors. *J. Am. Chem. Soc.* **2011**, *133*, 4447–4454.

24. Pirkle, A.; Chan, J.; Venugopal, A.; Hinojos, D.; Magnuson, C. W.; McDonnell, S.; Colombo, L.; Vogel, E. M.; Ruoff, R. S.; Wallace, R. M. The Effect of Chemical Residues on the Physical and Electrical Properties of Chemical Vapor Deposited Graphene Transferred to SiO_2. *Appl. Phys. Lett.* **2011**, *99*, 122108/1–122108/3.

25. Ryu, S.; Liu, L.; Berciaud, S.; Yu, Y.; Liu, H.; Kim, P.; Flynn, G. W.; Brus, L. E. Atomosheric Oxygen Binding and Hole Doping in Deformed Graphene on a SiO_2 Substrate. *Nano Lett.* **2010**, *10*, 4944–4951.

26. Li, L. J.; Shi, Y. M.; Kim, K. K.; Reina, A.; Hofmann, M.; Kong, J. Work Function Engineering of Graphene Electrode via Chemical Doping. *ACS Nano* **2010**, *4*, 2689–2694.

27. Huh, S.; Park, J.; Kim, K. S.; Hong, B. H.; Bin Kim, S. Selective n-Type Doping of Graphene by Photo-patterned Gold Nanoparticles. *ACS Nano* **2011**, *5*, 3639–3644.

28. Liu, Y. Q.; Liu, H. T.; Zhu, D. B. Chemical Doping of Graphene. *J. Mater. Chem.* **2011**, *21*, 3335–3345.

29. Das, A.; Pisana, S.; Chakraborty, B.; Piscanec, S.; Saha, S. K.; Waghmare, U. V.; Novoselov, K. S.; Krishnamurthy, H. R.; Geim, A. K.; Ferrari, A. C.; *et al.* Monitoring Dopants by Raman Scattering in an Electrochemically Top-Gated Graphene Transistor. *Nat. Nanotechnol.* **2008**, *3*, 210–215.

30. Casiraghi, C. Doping Dependence of the Raman Peaks Intensity of Graphene Close to the Dirac Point. *Phys. Rev. B* **2009**, *80*, 233407–233409.

31. Park, J.; Lee, W. H.; Huh, S.; Sim, S. H.; Kim, S. B.; Cho, K.; Hong, B. H.; Kim, K. S. Work-Function Engineering of Graphene Electrodes by Self-Assembled Monolayers for High-Performance Organic Field-Effect Transistors. *J. Phys. Chem. Lett.* **2011**, *2*, 841–845.

32. Berciaud, S.; Ryu, S.; Brus, L. E.; Heinz, T. F. Probing the Intrinsic Properties of Exfoliated Graphene: Raman Spectroscopy of Free-Standing Monolayers. *Nano Lett.* **2009**, *9*, 346–352.

33. Ni, Z. H.; Yu, T.; Luo, Z. Q.; Wang, Y. Y.; Liu, L.; Wong, C. P.; Miao, J. M.; Huang, W.; Shen, Z. X. Probing Charged Impurities in Suspended Graphene Using Raman Spectroscopy. *ACS Nano* **2009**, *3*, 569–574.

34. Suk, J. W.; Kitt, A.; Magnuson, C. W.; Hao, Y.; Ahmed, S.; An, J.; Swan, A. K.; Goldberg, B. B.; Ruoff, R. S. Transfer of CVD-Grown Monolayer Graphene onto Arbitrary Substrates. *ACS Nano* **2011**, *5*, 6916–6924.

35. Shi, Y. M.; Dong, X. C.; Chen, P.; Wang, J. L.; Li, L. J. Effective Doping of Single-Layer Graphene from Underlying SiO_2 Substrates. *Phys. Rev. B* **2009**, *79*, 115402–115405.

36. Lee, W. H.; Park, J.; Kim, Y.; Kim, K. S.; Hong, B. H.; Cho, K. Control of Graphene Field-Effect Transistors by Interfacial Hydrophobic Self-Assembled Monolayers. *Adv. Mater.* **2011**, *23*, 3460–3464.

37. Lafkioti, M.; Krauss, B.; Lohmann, T.; Zschieschang, U.; Klauk, H.; von Klitzing, K.; Smet, J. H. Graphene on a Hydrophobic Substrate: Doping Reduction and Hysteresis Suppression under Ambient Conditions. *Nano Lett.* **2010**, *10*, 1149–1153.

38. Farmer, D. B.; Golizadeh-Mojarad, R.; Perebeinos, V.; Lin, Y. M.; Tulevski, G. S.; Tsang, J. C.; Avouris, P. Chemical Doping and Electron–Hole Conduction Asymmetry in Graphene Devices. *Nano Lett.* **2009**, *9*, 388–392.

39. Schwierz, F. Graphene Transistors. *Nat. Nanotechnol.* **2010**, *5*, 487–496.

40. Chen, J. H.; Jang, C.; Adam, S.; Fuhrer, M. S.; Williams, E. D.; Ishigami, M. Charged-Impurity Scattering in Graphene. *Nat. Phys.* **2008**, *4*, 377–381.

41. Tan, Y. W.; Zhang, Y.; Bolotin, K.; Zhao, Y.; Adam, S.; Hwang, E. H.; Das Sarma, S.; Stormer, H. L.; Kim, P. Measurement of Scattering Rate and Minimum Conductivity in Graphene. *Phys. Rev. Lett.* **2007**, *99*, 246803–246806.

42. Adam, S.; Hwang, E. H.; Galitski, V. M.; Das Sarma, S. A Self-Consistent Theory for Graphene Transport. *Proc. Natl. Acad. Sci. U.S.A.* **2007**, *104*, 18392–18397.

43. Chen, W.; Chen, S.; Qi, D. C.; Gao, X. Y.; Wee, A. T. S. Surface Transfer p-Type Doping of Epitaxial Graphene. *J. Am. Chem. Soc.* **2007**, *129*, 10418–10422.

44. Yokota, Y.; Takai, K.; Enoki, T. Carrier Control of Graphene Driven by the Proximity Effect of Functionalized Self-Assembled Monolayers. *Nano Lett.* **2011**, *11*, 3669–3675.

45. Wang, R.; Wang, S. N.; Zhang, D. D.; Li, Z. J.; Fang, Y.; Qiu, X. H. Control of Carrier Type and Density in Exfoliated Graphene by Interface Engineering. *ACS Nano* **2011**, *5*, 408–412.

46. Yan, Z.; Sun, Z. Z.; Lu, W.; Yao, J.; Zhu, Y.; Tour, J. M. Controlled Modulation of Electronic Properties of Graphene by Self-Assembled Monolayers on SiO_2 Substrates. *ACS Nano* **2011**, *5*, 1535–1540.

47. Sakai, H.; Takahashi, Y.; Murata, H. Organic Field Effect Transistors with Dipole-Polarized Polymer Gate Dielectrics for Control of Threshold Voltage. *Appl. Phys. Lett.* **2007**, *91*, 113501/1–113501/3.